



First order magnetization processes in R_2Fe_{17} compounds ($R = Tb, Er$)

K.P. Skokov^{a,b,*}, Yu.G. Pastushenkov^b, Yu. Skourski^a, A.G. Khokholkov^b,
M.B. Lyakhova^b, S.S. Smirnov^b, K.-H. Müller^a

^a Leibniz-Institute for Solid State and Materials Research, 01171 Dresden, Germany

^b Physics Department of Tver State University, 170000 Tver, Russia

Abstract

Magnetization curves of both Er_2Fe_{17} and Tb_2Fe_{17} were measured on single crystals along the c-axis in the temperature range of 5-350 K and in a magnetic field up to 160 kOe. Two simulation techniques were used for micromagnetic modeling of magnetization curves of these compounds: (I) a vector-moment model and (II) a method based on the Neel-phase approach. Both simulation methods lead to identical results for the “regular” anisotropy types “easy axis”, “easy cone” and “easy plane”. However, in the case of a metastable anisotropy energy minimum along the c-axis the used simulation methods yield different results. Sets of anisotropy constants $K_1(T)$, $K_2(T)$ of Tb_2Fe_{17} and Er_2Fe_{17} were obtained using both simulation approaches for the temperature range 5÷300 K

© MISM2005. All rights reserved

PACS: 75.30.GW; 75.60.-d

Keywords: Magnetic anisotropy; Magnetisation curves; FOMP; Domain structure

Magnetic anisotropy constants K_1, K_2, \dots, K_n of a ferro- or ferrimagnet can be found from magnetization curves measured along various crystallographic directions. This method is based on fitting of an experimental magnetization curve $I_{exp}(H)$ by a calculated dependence $I_{calc}(H)$, where K_1, K_2, \dots, K_n are fit parameters. The values providing the best fit are considered as experimentally obtained. It is important to build a relevant expression for $I_{calc}(H)$ reflecting the real magnetization processes.

(I) The commonly used method of calculating $I_{calc}(H)$ is a vector-moment model. In this case $I_{calc}(H)$ is simulated by rotation of the spontaneous

magnetization I_s under applying an external magnetic field H [1,2]. Here a single-domain state of a sample is supposed. The magnetization value I is a projection of I_s onto the direction of external magnetic field H . The angle between the external field H and the vector I_s can be found minimizing the total energy E_{total} . It consists of the anisotropy energy and the energy of a magnetic moment in an external magnetic field. The advantage of this technique is its simplicity.

(II) On the contrary, Neel's phases method is based on the assumption that a sample can be subdivided into magnetic domains in low magnetic fields. Thus, the total energy E_{total} should include the

* Corresponding author. Tel.: +7-082-231-9327; fax: +7-0822-321274; e-mail: Skokov_K_P@mail.ru.

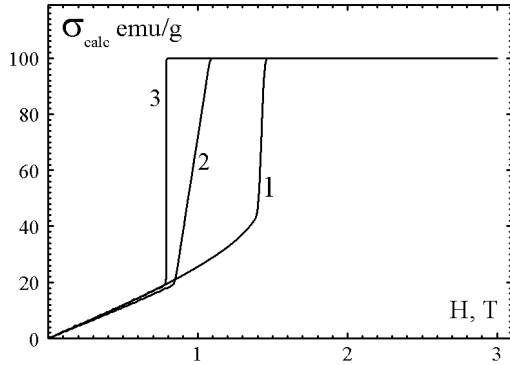


Fig 1. The simulated magnetization curves. (1) is calculated by the method of magnetization vector rotation (I), (2) calculated using the method of Neel phases (II), (3) is obtained from (2) by subtracting the demagnetisation field of a sample.

energy of the demagnetizing field of a specimen. In this case all the domains contribute to the projection of the magnetization on an external field direction. The advantage of the Neel's phases method is a more detailed description of magnetization processes [3-5].

Both simulation methods lead to identical results for the "regular" anisotropy types "easy axis", "easy cone" and "easy plane". However, in the case of a metastable anisotropy energy minimum, which shows up as a first order magnetization process (FOMP), those simulation methods yield different results. The background of this discrepancy is the appearance of a magnetic domain-like structure in the region of a FOMP-transition. Neel's phases technique should work much better in this case.

Fig.1 illustrates the differences between the two

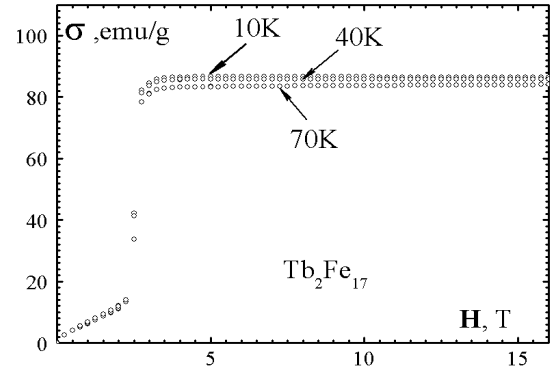


Fig 2. The magnetization curves measured along the crystallographic axis "c" of the single crystal Tb_2Fe_{17} at temperatures 10, 40, 70 K

methods near a FOMP. There $I_{calc}(H)$ are plotted for an arbitrary set of the anisotropy constants ($K_1=5 \times 10^6$ erg/cm³, $K_2 = -1 \times 10^7$ erg/cm³). The curve 1 is calculated by the method of magnetization vector rotation (I), curve 2 is obtained using the method of Neel's phases (II), and curve 3 is the same as curve 2 but with demagnetizing field subtracted. Curves 1 and 3 show an essential divergence.

To study the differences between the methods (I) and (II) experimentally, magnetization measurement of single crystals of Tb_2Fe_{17} and Er_2Fe_{17} were performed.

The starting ingot was prepared by inductive melting of the pure components. It was cooled down at a rate of 50-70 K/min and then subjected to a homogenization heat treatment (5h at 1170-1185°C). This procedure was chosen in order to provide

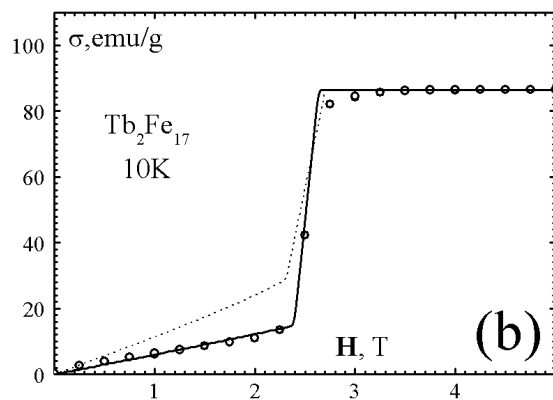
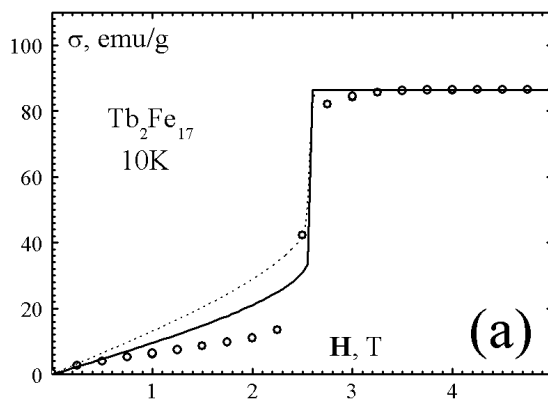


Fig 3. Experimental magnetization curves (circles) for the Tb_2Fe_{17} single crystal and the results of fitting by the method (I) (a) and (II) (b).

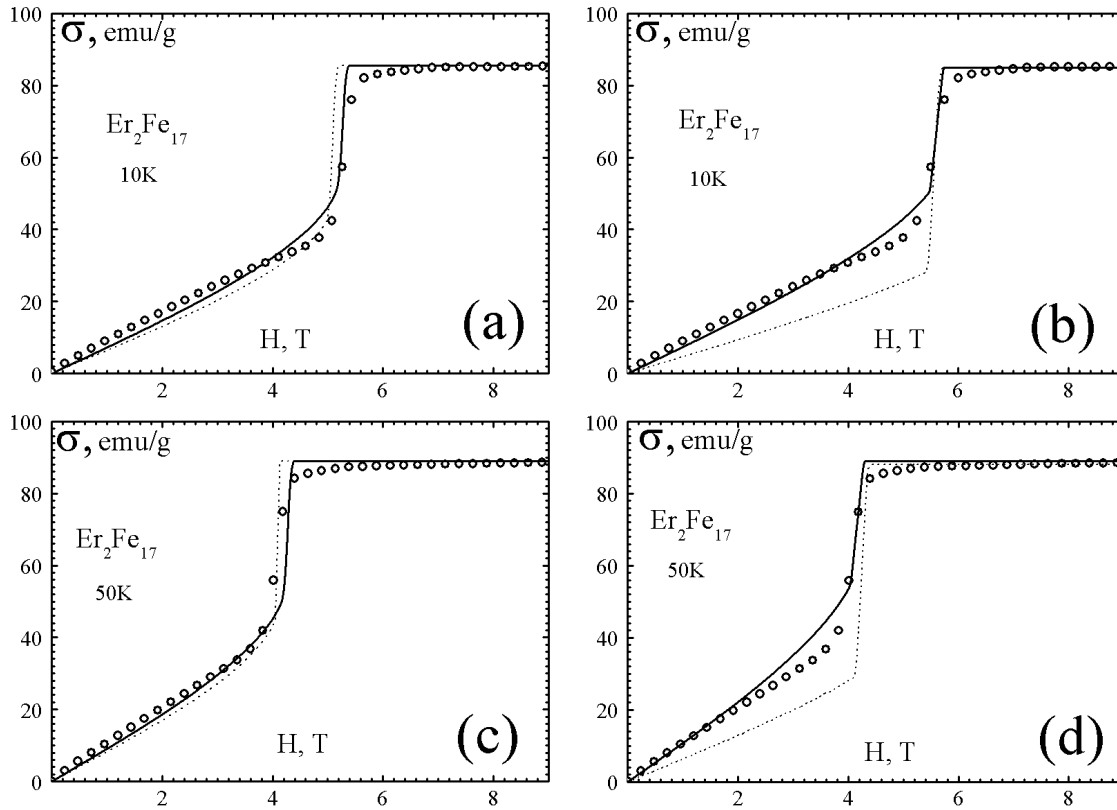


Fig. 4. Experimental magnetization curves (circles) measured at 10K (a,b) and 50K (c,d) for the $\text{Er}_2\text{Fe}_{17}$ single crystal and the results of the fitting by the method (I) (a,c) and (II) (b,d).

favorable conditions for growing large enough single crystalline grains.

Magnetic measurements were performed in a commercial SQUID magnetometer (Quantum Design MPMS-SS) and in a home made extractor magnetometer. Magnetization curves of both materials were measured along the *c*-axis in the temperature range of 5-350 K and in a magnetic field up to 160 kOe. In $\text{Tb}_2\text{Fe}_{17}$ the FOMP was observed below 100 K in a magnetic field range 25÷30 kOe. In $\text{Er}_2\text{Fe}_{17}$ this transition occurs in magnetic fields of 20÷50 kOe and also disappears at about 100 K.

The magnetization curves measured along the crystallographic *c*-axis of the single crystal of $\text{Tb}_2\text{Fe}_{17}$ at temperatures 10, 40, 70 K are shown at fig 2. Similarly to the results reported in [6, 7], no significant temperature dependence of the field of the FOMP transition was observed in a wide range of temperatures. However, the value of this field differs from that reported in previous studies [6, 7]. In our case this value is about 25 kOe, whereas in work [6]

this field is 50 kOe and in work [7] reports it to be 35 kOe. These differences could be explained by the following. The phase diagram of the 2:17 structure has a certain area of homogeneity. In our experiment, the range of homogeneity varied from $\text{R}_{1.96}\text{Fe}_{17}$ to $\text{R}_{2.06}\text{Fe}_{17}$ depending on the annealing temperature of the ingots. It makes it possible to tailor the field of the FOMP varying the ratio of Fe and R concentrations. The FOMP field decreases as the Fe concentration is increased. Additionally, no sign of a second jump on a magnetization curve which was reported in [6,7], was observed in the present study.

Experimental magnetization curves (circles) of the $\text{Tb}_2\text{Fe}_{17}$ single crystal measured at 10K are shown in Fig. 3. The results of the fitting of the magnetization curve using the method (I) are represented in Fig. 3(a). The solid line shows a curve calculated using $K_1 = 3.07 \times 10^7 \text{ erg/cm}^3$ and $K_2 = -3.16 \times 10^7 \text{ erg/cm}^3$. The dotted line shows a simulated magnetization curve obtained using $K_1 = 0$ and $K_2 = -1.18 \times 10^7 \text{ erg/cm}^3$. Despite the fact that the

FOMP fields for these curves coincide, the low field behavior of the simulated and the experimental curves show a notable discrepancy.

The results of fitting by the method (II) are shown in Fig. 3 (b). The solid curve is the result of a simulation with parameters $K_1 = 2 \times 10^7$ erg/cm³ and $K_2 = -3.5 \times 10^7$ erg/cm³, the dotted line shows a curve simulated with parameters $K_1 = 0$, $K_2 = -1.25 \times 10^7$ erg/cm³. Fig. 3 shows a good agreement of the simulated results and the experimental data.

Fig. 4 shows experimental magnetization curves of Er₂Fe₁₇ (all circles) measured at temperatures of 10K (a, b) and 50K (c, d). Fig. 4(a) presents the results of fitting of the magnetization curve using the method (I). The solid line is the simulation curve with parameters values $K_1 = -9.82 \times 10^6$ erg/cm³ and $K_2 = -1.63 \times 10^7$ erg/cm³. The dotted line shows the magnetization curve simulation with parameters $K_1 = 9.9 \times 10^5$ erg/cm³ and $K_2 = -2.4 \times 10^7$ erg/cm

The first set of anisotropy constants corresponds to the “easy plane” type of anisotropy. The second set is a combination of “easy plane” with a “metastable easy axis” anisotropy type. That means, that the method (I) can fit the experimental magnetization curve with two different parameter sets thus yielding ambiguous results. The same situation is observed at 50 K (Fig 4(c)). The solid and dotted lines were obtained with the parameters ($K_1 = -1.65 \times 10^6$, $K_2 = -1.45 \times 10^7$) and ($K_1 = 8 \times 10^5$, $K_2 = -2.05 \times 10^7$), correspondingly. Again, a good agreement using quite different parameter sets is observed.

The results of fitting by the method (II) are shown in Fig. 4 (b, d). The dotted line shows curves from a combination of “easy plane” with a “metastable easy axis” anisotropy type. The values of the parameters for Fig. 4(b): $K_1 = 0$, $K_2 = -3.2 \times 10^7$, and for the Fig. 4 (d) $K_1 = 0$, $K_2 = -2.5 \times 10^7$. However, the most accurate fit is represented by the solid lines. It is the result of the simulation with parameters $K_1 = -1.5 \times 10^7$ and $K_2 = -1.2 \times 10^7$, (b) and $K_1 = -1.15 \times 10^7$ and $K_2 = -8.5 \times 10^6$ (d). In this case, the simulation curves corresponding to the different anisotropy type are clearly distinguishable.

Acknowledgements

This work has been supported by Federal Program on Support of Leading Scientific Schools No 205.2003.03, grant RFBR No.05-02-17197 and grant

UR 01.01.054.

References

- [1] E.C.Stoner, E.P.Wohlfarth, Phil.Trans.Roy.Soc. 240 (1948) 599.
- [2] G. Asti., Ferromagnetic materials. 5. (1990) 397
- [3] L. J. Neel, Phys. Radium. 241 (1944) 51
- [4] H. Lawton, K.H.Stewart, Proc. R.Soc. 72 (1948) 88
- [5] R.R. Birss, D.J. Martin, J.Phys.C. 8 (1975) 189
- [6] X.C.Kou, F.R. de Boer, R. Grossinger, G. Wiesinger, H.Suzuki, H.Kitazawa, T.Takamasu, G.Kido, J. Magn. Magn. Mater. 177-181 (1998) 1002
- [7] I.S. Tereshina, S.A.Nikitin, K.P.Skokov, T.Palevski, V.V.Zubenko, I.V.Telegina, V.N.Verbesky, A.A.Salamova J. Magn. Mater. 350 (2003) 264